Supplementary Information

Co-Pt bimetallic nanoparticles with tunable magnetic and electrocatalytic properties prepared by Atomic layer deposition

Yan-Qiang Cao,[ab] Tao-Qing Zi,[a] Chang Liu,[a] Da-Peng Cui,[a] Di Wu,[a] and Ai-Dong Li*[a]*

[a]National Laboratory of Solid State Microstructures, Materials Science and Engineering Department, College of Engineering and Applied Sciences, Collaborative Innovation Center of Advanced Microstructures, Jiangsu Key Laboratory of Artificial Functional Materials, Nanjing University, Nanjing 210093, P. R. China

[b]Institute of Micro-nano Photonic & Beam Steering, School of Science, Nanjing University of Science and Technology, Nanjing 210094, P. R. China

Experimental details

Co-Pt bimetallic nanoparticles (BMNPs) preparation

Atomic layer deposition (ALD) processes were performed in a commercial flow-type hot-wall reactor (Picosun SUNALE R-150B). Si wafer with 300 nm thermally grown SiO_2 were used as substrates. Co_3O_4 and Pt were deposited by ALD using alternating doses of $CoCp_2$ (99%, Nanjing ai mo yuan Scientific equipment Co., Ltd.) and O_3 for Co_3O_4 at 250 ^oC, $(MeCp)PtMe_3$ (99%, Strem Chemicals) and O_2 for Pt at 300 ^oC. The $CoCp_2$ and $(MeCp)PtMe_3$ precursors were kept at 85 ^oC and 75 ^oC, respectively. High purity N_2 (5N) was used as carrier gas for all the precursors. The ALD sequence of Co_3O_4 is consisted of 1 s $CoCp_2$ and 1.5 s O_3 dose, followed by 5 s and 10 s N_2 purging, respectively. The typical Pt ALD cycle contained 0.2 s $(MeCp)PtMe_3$ and 1 s O_2 dose with by 5 s and 10 s N_2 purging, respectively. Various cycles of Co_3O_4 (100, 200, 300) and Pt (50, 100, 150, 200) were deposited in sequence. The growth rate of ALD Co_3O_4 is ~0.46 Å per cycle determined by ellipsometry. The thickness is 3.4, 8.3, and 12.7 nm for 100, 200, 300 cycles Co_3O_4. However, unlike oxide deposition, the ALD Pt exhibits the nucleation incubation mode.[1] Therefore, it's difficult to determine the thickness of Pt nanoparticles. Therefore the number of ALD cycles was used here instead of thickness. The as-

deposited Pt/Co_3O_4 bilayers were annealed in H_2 atmosphere (5% H_2-95% N_2) at 700 ^oC for 4 h with the ramp rate of 5 ^oC min^{-1}.

Materials characterizations

The surface chemical feature and composition was investigated by X-ray photoelectron spectroscopy (XPS, Thermo Fisher K-Alpha) with standard Al Kα (1486.7 eV) X-ray source. The binding energies were calibrated with respect to the signal from the adventitious carbon (binding energy = 284.6 eV). XPS was performed on two samples for each composition. The microstructure, morphology, and size distribution were examined by field emission scanning electron microscopy (FESEM, Ultra 55, ZEISS). Crystallinity and phase structures of the samples were analyzed by a Rigaku-D/MAX 2000 X-ray diffraction (XRD) system with Cu Kα radiation. The M-H curves were measured in a superconductivity quantum interference device magnetometer (SQUID-VSM, Quantum design) at room temperature. The applied magnetic field during measuring was parallel to the film.

Electrochemical measurements

For hydrogen evolution reaction (HER) activity test, Co-Pt BMNPs were deposited onto Toray carbon fiber paper (CFP, TGP-H-060). In order to well coat this 3D substrate, the dosing and purging time during ALD process was extended to 5 s and 30 s, respectively, for each precursor. Electrochemical measurements were performed

in a three-electrode electrochemical cell at room temperature using 1M KOH as the electrolyte. The Co-Pt BMNPs with various composition on CFP were used directly as the working electrodes. A Pt wire and Ag/AgCl were used as the counter electrode and the reference electrode, respectively. Linear sweep voltammograms (LSVs) were conducted using an electrochemical work station (CHI660E) with a scan rate of 5 mV s^{-1}. Electrochemical impedance spectra (EIS) were performed over a frequency range of 10^5-0.1 Hz at onset overpotentials of the catalysts with AC amplitude of 5 mV. The *iR* correction to data with the series resistance is done by the equation of $\eta_{corr} = \eta_{exp} - iR$. At least two samples were tested in HER for each composition.

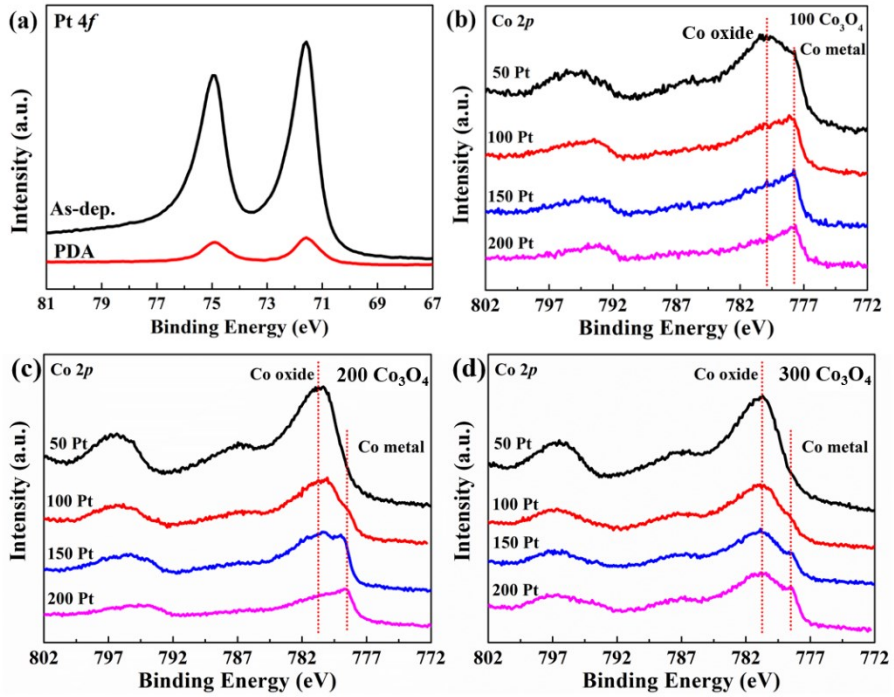

Fig. S1 (a) Pt 4f XPS spectra for the 100Co-200Pt before and after H_2 PDA. Co 2p XPS spectra for Co-Pt BMNPs formed after H_2 PDA with different Pt ALD cycles: (b) 100, (c) 200, and (c) 300 cycles Co_3O_4.

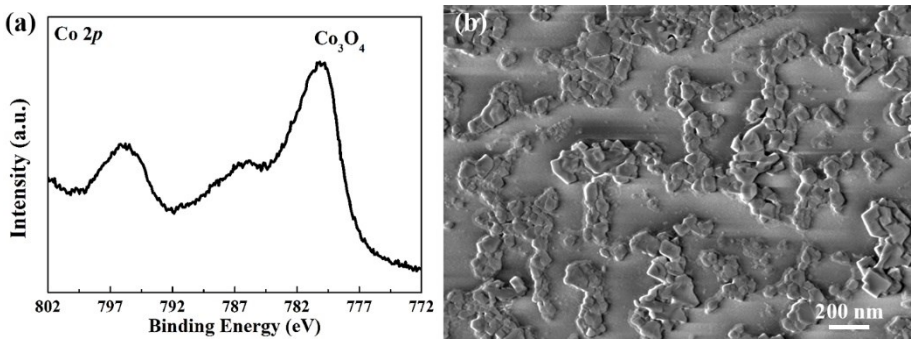

Fig. S2 (a) Co 2p XPS spectrum and (b) SEM image of Co_3O_4 (300 cycles) after H_2 PDA.

Unlike Co_3O_4/Pt bilayer, pristine Co_3O_4 only shrinks to form large grain after H_2 PDA process, as shown in Fig. S2(b). It has been widely demonstrated that ALD Pt exhibits island deposition model. The Pt clusters can work as the catalytic center for

the reduction reaction of Co_3O_4 to Co. Then, the reduced metal Co can migrate into Pt clusters to form Co-Pt BMNPs. Therefore, no nanoparticles were formed for pristine Co_3O_4 due to the lack of catalytic center.

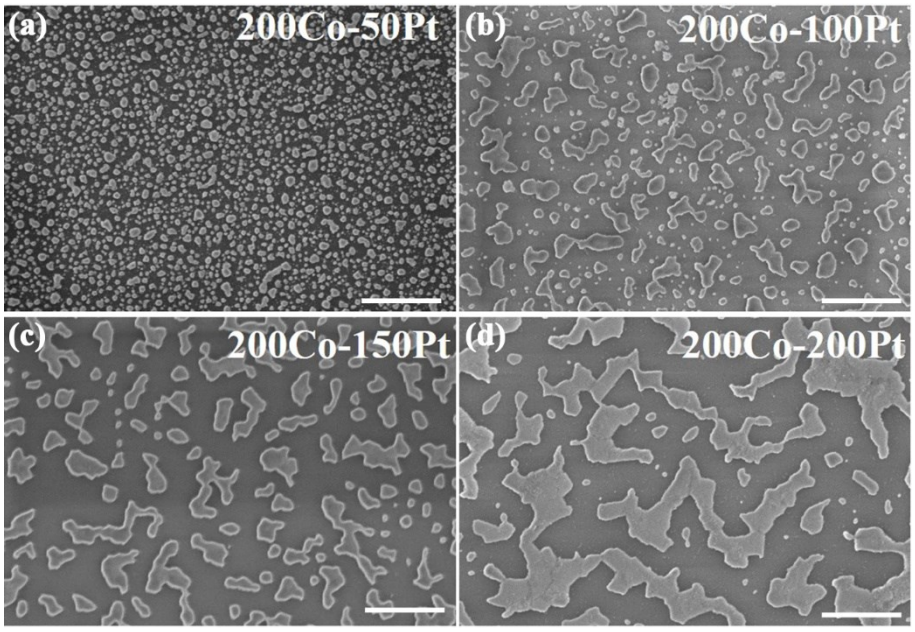

Fig. S3 SEM images of Co-Pt BMNPs with 200 cycles ALD Co_3O_4, varying ALD Pt cycles: (a) 50, (b) 100, (c) 150, and (d) 200. The scale bar is 1 um.

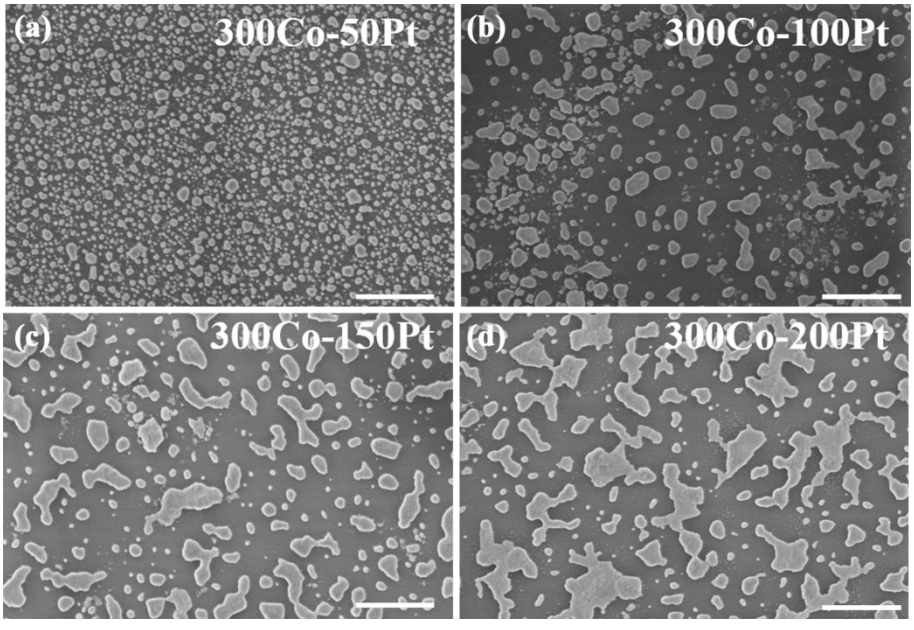

Fig. S4 SEM images of Co-Pt BMNPs with 300 cycles ALD Co_3O_4, varying ALD Pt

cycles: (a) 50, (b) 100, (c) 150, and (d) 200. The scale bar is 1 um.

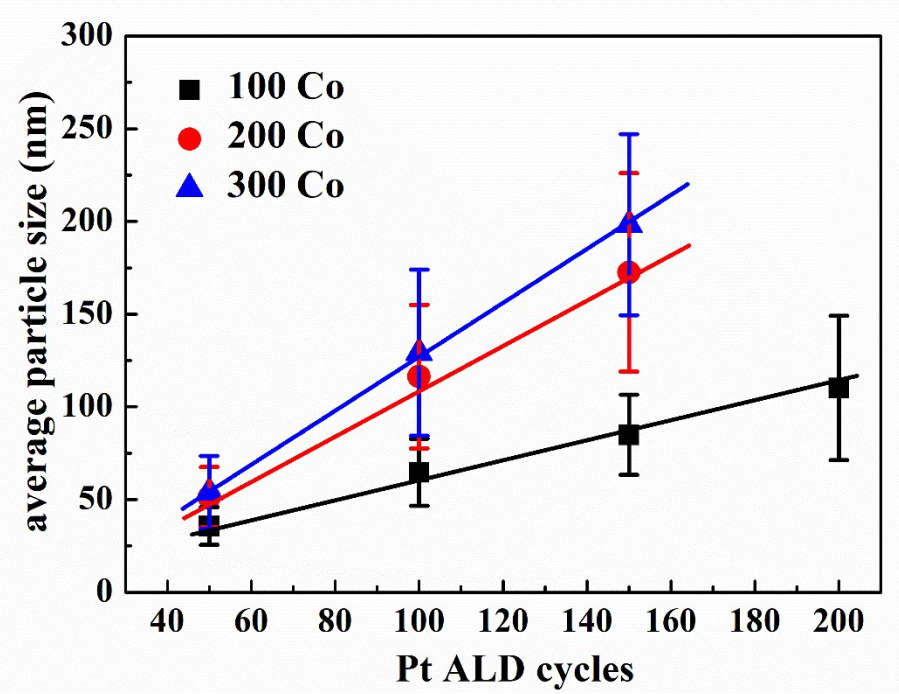

Fig. S5 Average particle size of Co-Pt BMNPs versus Pt ALD cycles.

For the thick sample (200Co-200Pt and 300Co-200Pt), the prepared Co-Pt BMNPs begin to aggregate together to form very large particles. Therefore, well dispersed nanoparticles can be formed when the parent Co_3O_4/Pt bilayer is thin. Based the statistical results in Fig. S5, the particle size of Co-Pt BMNPs can be fine tuned in the range of less than ~200 nm .

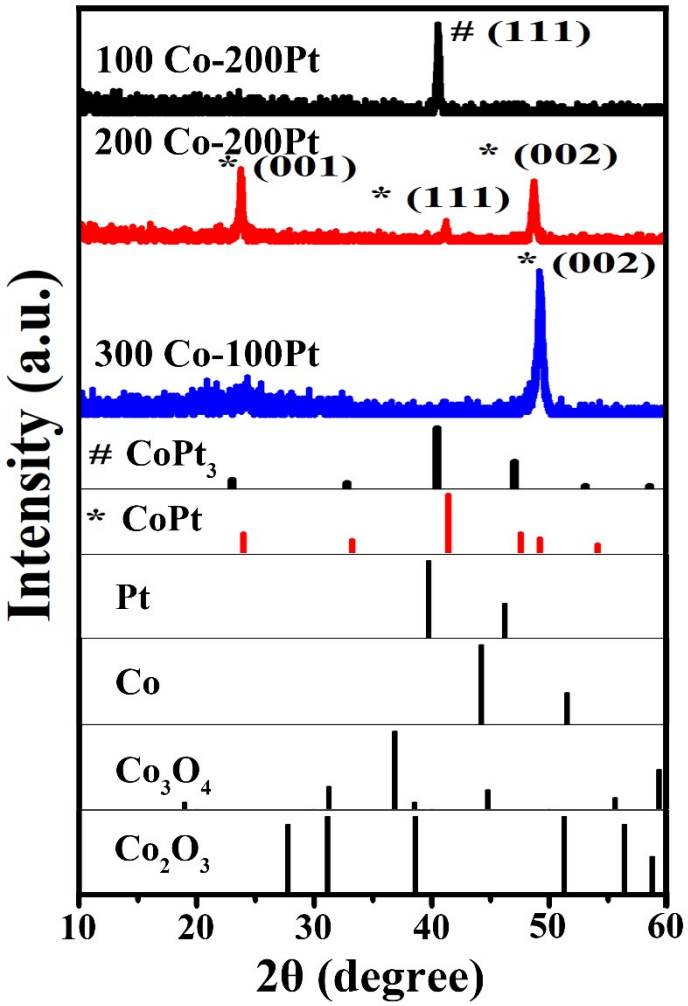

Fig.S6 XRD patterns of Co-Pt BMNPs with various composition. The theoretical peak positions of $CoPt_3$, CoPt, Pt, Co, Co_3O_4 and Co_2O_3 are also presented as reference.

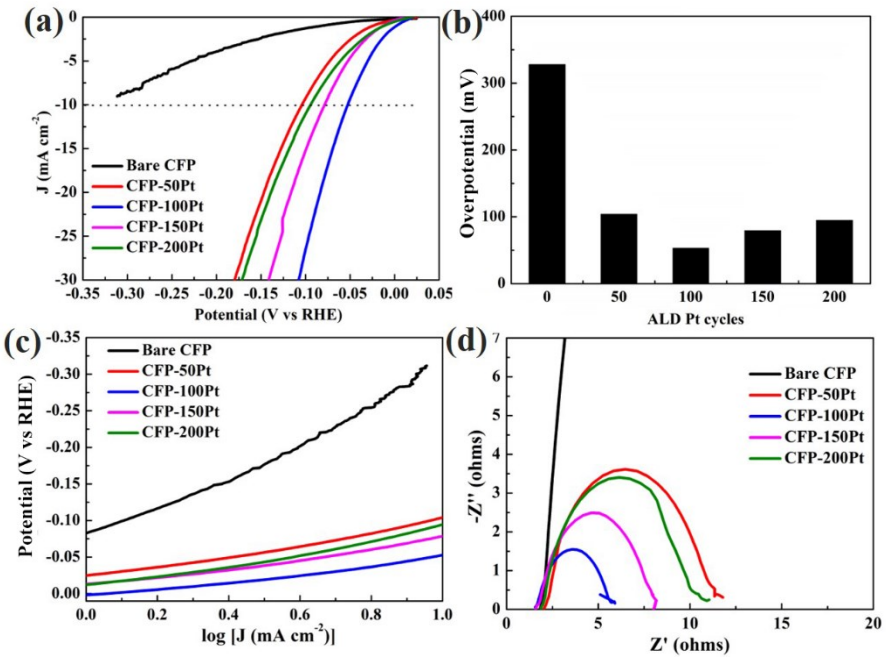

Fig. S7 Electrocatalytic performance of ALD Pt NPs with various cycles on CFP. (a) LSVs, (b) overpotentials vs. ALD Pt cycles, (c) Tafel plots, and (d) EIS.

It can be seen that bare CFP shows weak HER activity, exhibiting the overpotential > 300 mV at the current density of 10 mA cm^{-2}. After various ALD Pt deposition, the HER activity is improved greatly. 100 cycles ALD Pt coated CFP exhibits the best HER performance, including the lowest overpotential of 53 mV (10 mA cm^{-2}), Tafel slop of 51 mV dec^{-1}, and charge-transfer resistance.

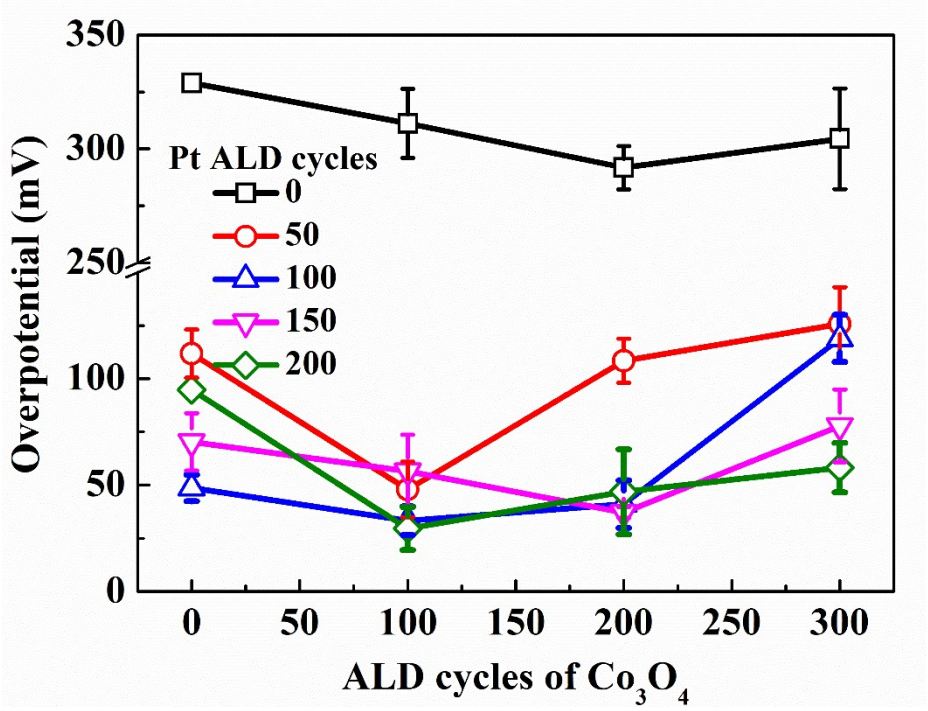

Fig. S8 Overpotential at 10 mA cm^{-2} for Co-Pt BMNPs with various composition.

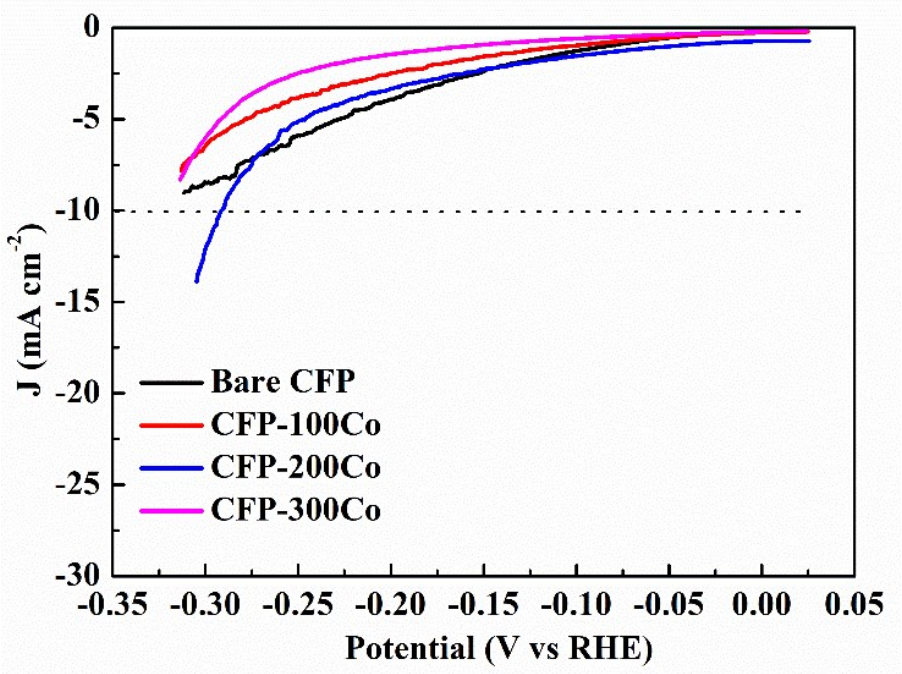

Fig. S9 LSVs for various ALD cycles Co_3O_4 on CFP.

Table S1 Coercivity of the ALD deposited materials measured at room temperature

Materials	coercivity (Oe)	Ref.
Fe_3O_4	213	2
Fe_3O_4	380	3
$CoFe_2O_4$	200-2200	4
cobalt carbide	500	5
$Ni_{83}Fe_{17}$	475	6
$BiFeO_3$	5	7
Fe_3O_4	390	8
Mn doped TiO_2	54	9
$CoFe_2O_4$	1500	10
Co nanorods	857	11
CoPt	1520	This work

References

1. X.-J. Liu, L. Zhu, M.-Y. Gao, X.-F. Li, Z.-Y. Cao, H.-F. Zhai, A.-D. Li and D. Wu, *Applied Surface Science*, 2014, **289**, 332-337.
2. L. Zhang, Z. Zhou, Y. Zhang, B. Peng, W. Ren, Z. Ye and M. Liu, *IEEE Transactions on Magnetics*, 2019, **55**, 1-7.
3. J. L. Palma, A. Pereira, R. Álvaro, J. M. Garcíamartín and J. Escrig, *Beilstein Journal of Nanotechnology*, 2018, **9**, 1728-1734.
4. C. D. Pham, J. Chang, M. A. Zurbuchen and J. P. Chang, *ACS Applied Materials & Interfaces*, 2017, **9**, 36980-36988.
5. M. Sarr, N. Bahlawane, D. Arl, M. Dossot, E. McRae and D. Lenoble, *Applied Surface Science*, 2016, **379**, 523-529.
6. A. P. Espejo, R. Zierold, J. Gooth, J. Dendooven, C. Detavernier, J. Escrig and K. Nielsch, *Nanotechnology*, 2016, **27**, 345707.
7. P. Jalkanen, V. Tuboltsev, B. Marchand, A. Savin, M. Puttaswamy, M. Vehkamäki, K. Mizohata, M. Kemell, T. Hatanpää, V. Rogozin, J. Räisänen, M. Ritala and M. Leskelä, *The Journal of Physical Chemistry Letters*, 2014, **5**, 4319-4323.
8. R. Zierold, C. L. Lam, J. Dendooven, J. Gooth, T. B?Hnert, P. Sergelius, F. Munnik,

J. M. Montero Moreno, D. G?Rlitz and C. Detavernier, *Journal of Physics D Applied Physics*, 2014, **47**, 485001.

9. M. C. K. Sellers and E. G. Seebauer, *Applied Physics A*, 2011, **104**, 583-586.
10. Y. T. Chong, E. M. Y. Yau, K. Nielsch and J. Bachmann, *Chemistry of Materials*, 2010, **22**, 6506-6508.
11. H. B. R. Lee, G. H. Gu, J. Y. Son, G. P. Chan and H. Kim, *Small*, 2008, **4**, 2247-2254.